



## The DTT device: First wall, vessel and cryostat structures



Giuseppe Di Gironimo<sup>a,\*</sup>, Domenico Marzullo<sup>a</sup>, Rocco Mozzillo<sup>a</sup>, Andrea Tarallo<sup>a</sup>,  
Fabio Villone<sup>b</sup>

<sup>a</sup> CREATE, University of Naples Federico II – DII, P.le Tecchio 80, 80125 Napoli, Italy

<sup>b</sup> CREATE, Università di Cassino e Lazio Meridionale – DIEI, Viale dell'Università, 03043 Cassino, FR, Italy

### HIGHLIGHTS

- Conceptual design and preliminary structural assessment of the FW, VV and cryostat of DTT device have been proposed.
- VV design resulted in an all-welded single-wall toroidal structure made of 18 sectors.
- FW consists of a bundle of tubes armoured with plasma-sprayed tungsten (W).
- Cryostat is conceived as a single-wall cylindrical vessel supported by a steel frame structure.

### ARTICLE INFO

#### Article history:

Received 28 July 2016

Received in revised form 21 March 2017

Accepted 30 April 2017

Available online 14 May 2017

#### Keywords:

Conceptual design  
3D CAD modeling  
Mechanical analysis  
FEM  
Vacuum vessel  
First wall  
Cryostat

### ABSTRACT

This paper describes the activity addressed to the conceptual design of the first wall and the main containment structures of DTT device. The work moved from the geometrical constraints imposed by the desired plasma shape and the configuration needed for the magnetic coils. Many other design constraints have been taken into account such as remote maintainability, space reservations for diagnostic and heating equipment, etc.

The basic vessel design resulted in an all-welded single-wall toroidal structure made of 18 sectors. Proper supports have been designed for the first wall, which was conveniently segmented in view of remote maintenance. This provisional model allowed evaluating the electromagnetic loads on the metallic structure of the vacuum vessel resulting from the current quench due to a plasma disruption.

After a FEA mechanical assessment, which was conducted according to ASME code, INCONEL<sup>®</sup> 625 has been provisionally selected as reference material for vacuum vessel. The design principles of the cryostat were chiefly based on cost minimization and functionality; thus it was conceived as a single-wall cylindrical vessel supported by a steel frame structure. The same structure will hold the vacuum vessel and the magnets.

© 2017 Elsevier B.V. All rights reserved.

## 1. Introduction

According to the European roadmap towards the development of fusion energy plants [1], a solid solution to the problem of heat exhaust is certainly one of the main challenges. Alternative solutions are indeed needed for the divertor system design to mitigate the risk that the conventional solutions tested in ITER may not extrapolate to DEMO.

From this point of view, the *Divertor TOKAMAK Test facility* (DTT) is conceived as bridge between today's proof-of-principle experi-

ments and DEMO. In particular, DTT will have the potential to bring alternative divertor solutions to a sufficient readiness level to be adopted on DEMO [2].

DTT will operate in parallel with ITER, likely before its high performance operations. Therefore, DTT will support and complement the ITER experimental program, paying particular attention to high priority issues like disruption avoidance/mitigation, R&D needs in plasma facing components, pacing of Edge Localized Modes (ELM), and plasma control [6]. In the frame of DTT project, the authors have been involved in the conceptual design and the very preliminary structural assessments of the vacuum vessel, the first wall and the cryostat structures.

The work moved from the geometrical constraints imposed by the desired plasma shape and the configuration needed for the magnetic coils. Many other design constraints have been taken

\* Corresponding author.

E-mail addresses: [giuseppe.digironimo@unina.it](mailto:giuseppe.digironimo@unina.it), [peppe.digironimo@gmail.com](mailto:peppe.digironimo@gmail.com) (G. Di Gironimo).

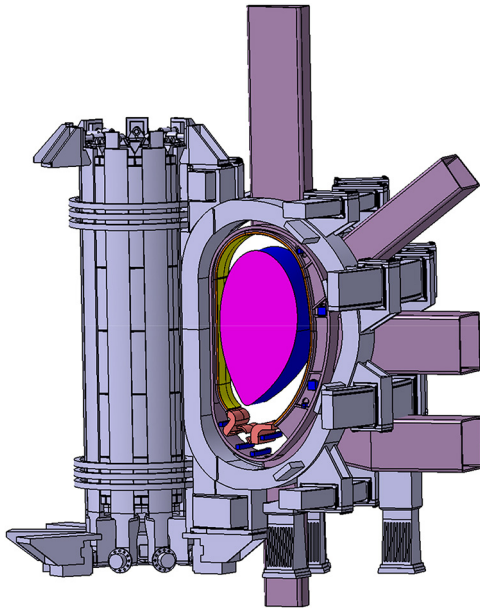


**Fig. 1.** Isometric view of a Vacuum Vessel sector with schematic representation of magnets and principal in-vessel components (FW and divertor).

into account such as remote maintainability, space reservations for diagnostic and heating equipment, etc. In order to investigate different geometrical configuration the DTT CAD design is based on a parametric approach [7].

The main design requirements and the results of our assessments are thus being discussed in the next sections.

## 2. The vacuum vessel and the first wall

The Vacuum Vessel (VV) will be located inside the main magnet system and will provide an enclosed, vacuum environment for the plasma. It will also act as a first confinement barrier. Its main components are the **main vessel**, the **port structures** and the **supporting system**. Moreover a **first wall** (FW) surrounds most of the inner vessel wall (Fig. 1). The main vessel is a torus with “D” shaped cross-section, segmented in 18 sectors, 20° wide each. The design of the VV shall meet the following main requirements:

- The main vessel shall provide a boundary consistent with the ultra-high vacuum (UHV) requirements;
- The main vessel shall support the in-vessel components (e.g. first wall, divertor system, etc.) in nominal and off-normal/fault operating conditions;
- The vacuum vessel, together with the in-vessel components, shall provide a specified toroidal electrical resistance (estimated in about 150  $\mu\Omega$ );
- In-vessel components shall be compatible with remote handling operations;
- The poloidal curvature of VV shall be consistent with the presence of the in-vessel coils;
- The main vessel shall be endowed with 5 access ports for each sector and feedthroughs for in-vessel components;
- The position and the geometry of the ports shall be consistent with both the poloidal and the toroidal field coils (TFCs) and their supporting structure;
- At least one port per sector must be aligned with plasma center;
- At least one port per sector shall allow for the (de) commissioning of the divertor;
- At least one port shall allow for the installation of a tangential neutral beam injection (NBI) system.

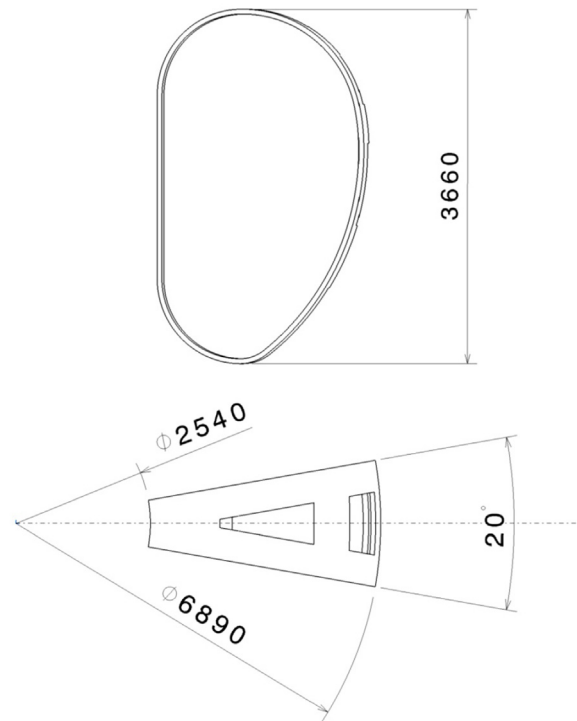


**Fig. 2.** Overall dimensions (in mm) of main vessel sector (top and side views).

**Table 1**

Main mechanical properties of AISI SS316L and Inconel®.

Property	AISI SS-316-L(N)	INCONEL® 625
Density [g/cm <sup>3</sup> ]	~8	~8,5
Module of Elasticity [GPa]	~200	~200
Yield strength [MPa]	~230	~400
Tensile strength [MPa]	~550	~800
Electrical Resistivity @ 20 °C [ $\mu\Omega$ cm]	~74	~130

The main vessel design is an all-welded single-wall structure. The 18 sectors are joined by field welding.

The maximum thickness of the shell is 35 mm. The VV profile in a poloidal plane is made by single curvature segments. Thus the resulting shell will have a double curvature at the outboard side and a single curvature at the inboard side, where the shells of the central segment are cylindrical. The shell shall be manufactured by hot forming/bending and welding. Given the single-shell design, a proper heat shield, similar to the one already provided for Wendelstein 7-X [4], will be subject of future studies. The heat shield will be designed in order that the VV achieves a reference temperature of 100 °C.

Overall external dimensions of the vacuum vessel are 3660 mm in height with a diameter of 2540 mm at the inboard side and a diameter of 6890 mm at the outboard side (Fig. 2).

The material choice for vacuum vessel has a significant influence on performance, fabrication characteristics, mechanical strength, chemistry properties, and construction cost. The primary candidate for the vacuum vessel material would be AISI SS-316L(N), owing to its large database and its fabricability by conventional technology. However, compared with AISI SS-316L(N), INCONEL® 625 has a higher electrical resistivity and better mechanical properties (Table 1).

Moreover, given the low irradiation levels [3], no significant decreasing in the main mechanical characteristics of Inconel 625 is expected [5].

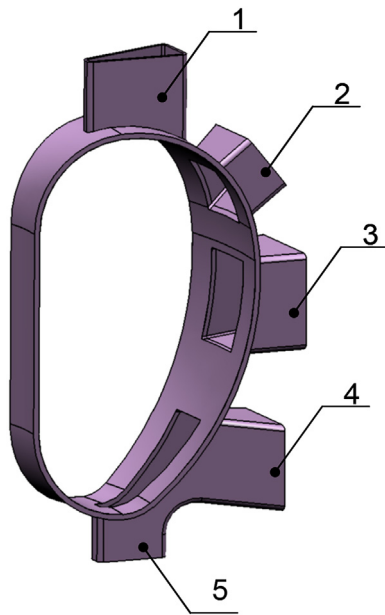


Fig. 3. DTT VV – 20° module with ports provisional numbering.

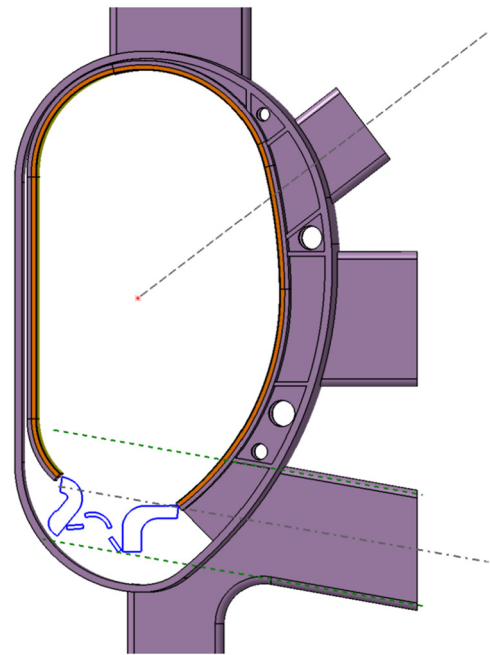


Fig. 4. Alignment of ports nr. 2 and nr. 4.

Therefore INCONEL<sup>®</sup> 625 has been provisionally selected as the reference material for the main vessel, though further investigations concerning manufacturing and costs issues are still needed based on the experience of the already existing fusion plants that use INCONEL<sup>®</sup> as material for vacuum vessel [8].

As mentioned, VV shall provide several openings for the plasma diagnostic systems, vacuum systems, the auxiliary heating system, the in-vessel Remote Handling (RH) maintenance system, etc.

A minimal clearance of 100 mm between VV and the magnetic coils has been left to house proper neutral and thermal shields (not presented in details at the current stage of the design).

### 2.1. Access ports

As mentioned, each vessel sector is equipped with 5 access ports that will be used for the maintenance and the replacement of the in-vessel components (divertor cassette, first wall) and for the allocation of diagnostic and heating equipment (Fig. 3). Access ports have been conceived as single-walled structures welded to the main vessel. Their thickness has been provisionally determined in 25 mm. It is understood that further structural analyses shall be conducted to optimize this thickness. Proper bellows shall accommodate for small movements along the port axis.

As required, port nr. 2 is aligned to see plasma center (Fig. 4).

In order to ease the access to divertor for remote maintenance or its (de)commissioning, access port nr. 4 is aligned with a possible divertor exit path (Fig. 4). This choice implies that ports nr. 4 and nr. 5 will converge in a single opening on the main vessel (Fig. 5).

The equatorial ports (port nr. 3) are generally characterized by an opening shape relatively high and rather narrow. However, the NBI system is planned to consist of two units, one perpendicular and one tangential. Therefore, at least one of the equatorial ports must be one-side enlarged to accommodate the co-tangential unit of the NBI system (Fig. 6).

Since the beams are injected at 45° relative to the magnetic axis, the port available space is reduced. This configuration has been chosen to assure the best compromise between the narrow spaces available and the 10 MW of power which is to be supplied. It is worth noticing that, with this choice, the geometry of the first wall is not affected by the presence of NBI system.

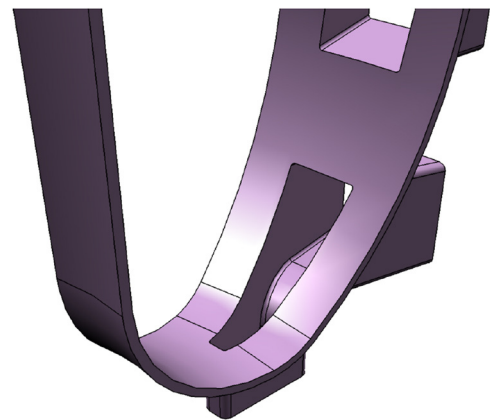


Fig. 5. Lower ports converge in a single opening on the main vessel.

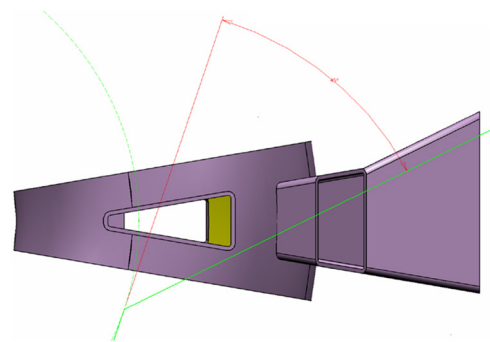


Fig. 6. Enlarged equatorial port aimed at accommodating the co-tangential NBI beam.

### 2.2. Vessel supports

The VV will be vertically supported by elastic supports resting directly on the ring pedestal (Fig. 7). An example of such a design solution can be found in [9]. These supports will be radially restrained against fast displacements taking place during seismic

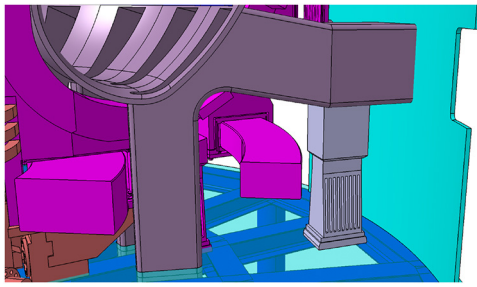


Fig. 7. VV support concept.

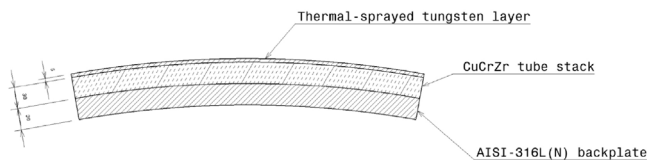


Fig. 8. First wall layers.

events or fast transients. However, they shall be free to move radially to allow for thermal expansion. The VV is also restrained vertically in the upward direction through a set of vertical links, located between the pedestal and the lower port. Additionally, the VV will be restrained in a toroidal plane for the position centering. The toroidal restraints shall be made of special springs between the VV ports and pedestal ring. These toroidal supports shall maintain the horizontal relative position between the VV and the TF Coil. They can also reduce loads on the vertical supports and make sure that the two systems, the VV and the TFC, resonate in unison and maintain their relative displacement well below the allocated gap during a seismic event and/or VDE.

### 2.3. First wall

Heat loads on the first wall in normal operation include radiation and particle bombardment from the burning plasma. The power transported by neutrals from charge-exchange is important only locally near neutral particle sources for fuelling. A maximum thermal load of  $3 \text{ MW/m}^2$  is expected on the equatorial inboard side of the FW [3]. Based on previous studies [10], the FW shall consist of a bundle of tubes armoured with plasma-sprayed tungsten (W). The plasma facing tungsten is about 5 mm thick (except for the equatorial and upper inboard segments where the tungsten layer is about 10 mm thick), the bundle of stainless steel tubes (coaxial pipes in charge of cooling operation) is 30 mm thick, and the backplate supporting the tubes is 30 mm thick of SS316L(N) (Fig. 8).

During start-up and disruptions, abnormal loads are experienced in addition when the first wall acts as a limiter and from the impact of run-away electrons. For this reason, the tungsten layer is doubled at the upper and equatorial inboard side, where higher thermal loads are expected.

The definition of the curvature on a poloidal plane meets the necessity to optimize the space available for the plasma within the chamber, especially in the inner part of the chamber. Indeed, in several scenarios with diverted configuration, and mainly after an L-H transition, the shape controller needs to counteract plasma drift phenomena towards the Central Solenoid and avoid plasma disruptions, caused by contacts with surrounding physical structures and yielding a sudden loss of confinement and energy content. Apart from the controller response times, plasma-wall clearance can be minimized by leaving plasma as much available volume as possible, which means a placing of the FW as close as possible to the VV, except for a minimum tolerance to fill with the supporting

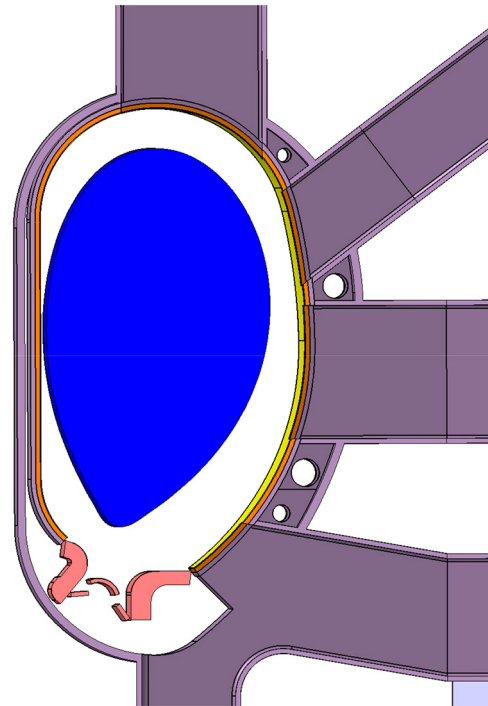


Fig. 9. DTT FW profile.

structure (Fig. 9). Furthermore, the poloidal curvature needs to take into account the presence of the in-vessel coils, placed between the equatorial and the vertical ports and exploited for magnetic control purposes (Edge Localized Modes, vertical stability, radial position) [10].

The radioactivity induced by neutrons has an impact on maintenance operations and waste management. A not negligible activation at short-medium times after DTT shutdown is expected especially in plasma-facing components. The estimated contact dose rate level at 1 day at the end of DTT operations is indeed  $\sim 100 \text{ mSv/h}$  in tungsten. At longer cooling times, higher induced radioactivity is observed in steel mainly because of nickel, cobalt, and tantalum activation (i.e.  $\sim 10 \text{ mSv/h}$  in VV at one month after shutdown), therefore remote handling is mandatory. The radioactivity level may require the preparation of an ad hoc temporary repository to store some of the dismantled activated components. However, within 50 years from the shutdown, the contact dose of all components should be  $< 10 \mu\text{Sv/h}$ , and the level of activity should not cause waste management problems [3]. The feasibility of a remote maintenance via the equatorial port is a main requirement of FW design, since many FW components are expected to have to be maintained at some stage. Therefore, a proper modular design for the FW must be provided to allow for its dismantling through the equatorial port by means of a proper robot manipulator. Fig. 10 depicts a possible conceptual segmentation of the FW, yet compatible with the motion simulations through the equatorial port. At the current stage, 15 modules per sector are provided.

The physical separation between adjacent modules is obtained via the introduction of a 5 mm clearance. However, further studies should be conducted on FW support structure to better define their modular design.

#### 2.3.1. Support structure for the first wall

As mentioned, the plasma-facing FW panel is supported by a backplate that will be joined to the vacuum vessel through a mechanical attachment system of flexible supports and a system of keys. However, at the outboard side, the first wall is about 200 mm

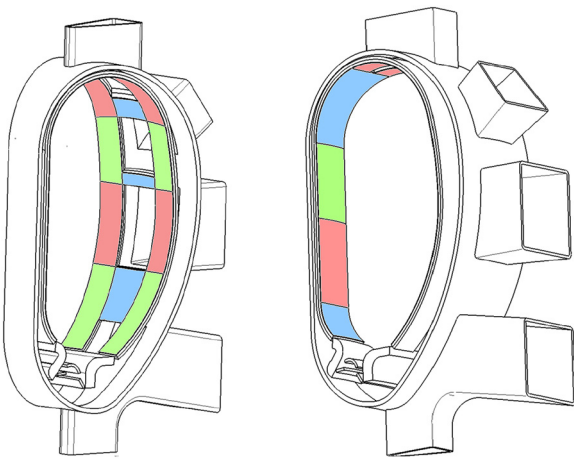


Fig. 10. Provisional FW segmentation in poloidal plane.

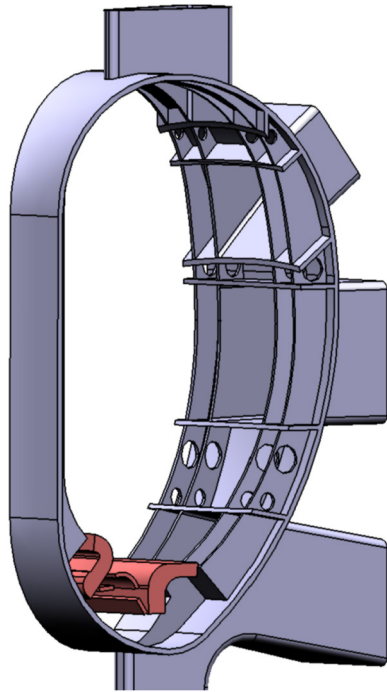


Fig. 11. Conceptual FW support structure at outboard side of the vacuum chamber.

far from the vacuum chamber internal surface. This implies that a suitable structure must be designed capable to support the backplate. The provisional solution is shown in Fig. 11.

The structure is made of 4 poloidal ribs and 6 toroidal ribs per sector. The toroidal ribs along with the two inner poloidal ribs stand in correspondence to the ports side-walls in order to help to strengthen the vessel. Several lightening holes were provided to also house and support the internal toroidal coils. This structure also provides the electrical connection between backplate and the vacuum vessel. It is clear that the mentioned structure shall be detailed according to the joint mechanism between backplate and FW and supports as well as to the maintenance requirements. Moreover, supports could be locally reinforced to face abnormal loads, coming from plasma start-up and disruptions.

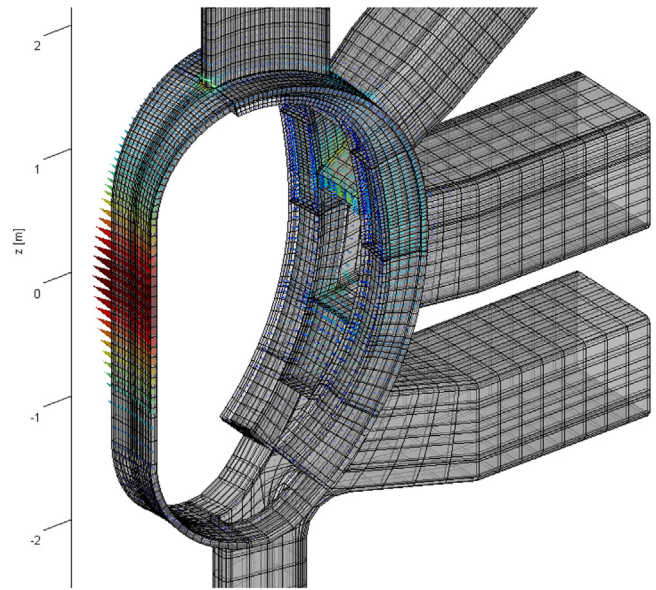


Fig. 12. Typical eddy current density pattern induced in the vessel.

#### 2.4. Design justification and preliminary finite element analysis

A FE stress analysis on the main vessel was conducted with ANSYS 2015 to validate the thicknesses and the material provisionally defined and to identify possible critical areas.

The operating scenarios of the VV are characterized by loads which are quite low during normal plasma behaviour and rather large during plasma VDE [11] and disruptions. The worst disruption expected for the VV is a strong vertical asymmetric VDE.

We assumed a VDE model where the vertical displacement of the plasma column is followed by a sudden loss of the plasma thermal energy (when the *safety factor q* goes below 1.5) and then by a fast current quench (1.5 MA/ms).

The electromagnetic loads on the vacuum vessel due to the current quench in a plasma disruption have been computed considering a filament (at  $R = 2.15$  m,  $Z = 0.15$  m) that simulates the plasma. Its current decreases linearly from 6 MA to 0 in 5 ms, which is the current quench time coming from the scaling proposed in [12]. Simultaneously, the plasma toroidal flux is supposed to decrease from 0.3 Wb to zero in the same interval. The magnetic field has both a poloidal and a toroidal component, which is supposed to have an ideal  $1/r$  spatial dependence, with a value of 6 T at 2.5 m. The eddy currents induced in the vessel (Fig. 12) interact with the magnetic field, giving rise to the electromagnetic loads (Fig. 13), which have been computed with the CARIDDI code [13]. A positive validation of the simplifying assumptions has been carried out with a more detailed computational model, including a self-consistent description of the plasma movement [14]. The maximum values of forces and torques acting on one sector of the structure are reported in Table 2, where  $x, y, z$  refer to a global Cartesian coordinate system and the torques are computed with respect to the origin of such system.

The simulation model comprehends the main vessel (35 mm), the port structures (25 mm), the FW supports (25 mm) and the FW backplate (30 mm). The electromagnetic loads due to the worst VDE at the time of their maximum values were considered as an external forces field applied to the vessel structures. Moreover the dead load of the Vacuum Vessel has been taken into account.

The constraints have been placed on the external edge of lower port to allow rotations in  $x-z$  planes and thermal deformation in radial direction.

**Table 2**  
Maximum values of forces and torques acting on one sector of the structures.

Material	Max Fx  [kN]	Max Fy  [kN]	Max Fz  [kN]	Max Mx  [kN m]	Max My  [kN m]	Max Mz  [kN m]
Vessel	939.7	6.8	85.7	125.0	382.7	8.6
Port extension	267.5	16.9	10.4	409.0	90.4	7.1
Support	46.2	7.8	26.7	620.3	125.1	2.1
Backplate	45.9	10.2	30.6	75.7	76.4	1.7
Cooling plate	9.5	5.1	7.9	62.6	17.8	0.4
First wall	152.5	7.9	39.1	6.2	120.4	1.4

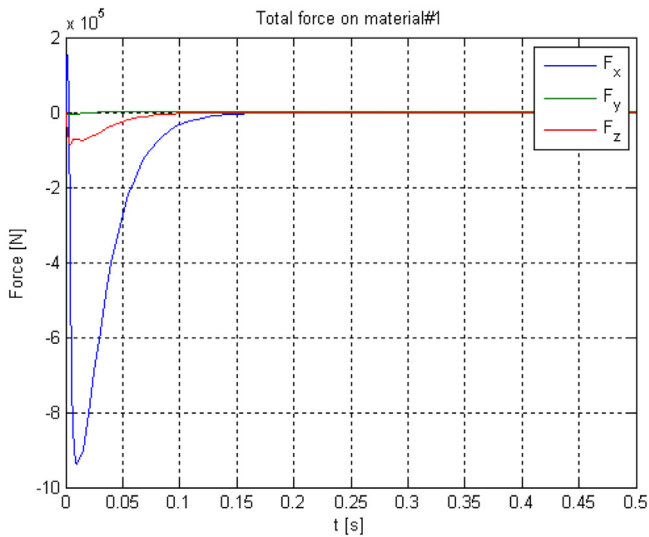


Fig. 13. Resultant force acting on one sector of the vessel.

The material proprieties for INCONEL® 625 [3] have been referred to a temperature of 100 °C. The allowable stress is  $S_m = 265$  MPa.

Our analyses showed that, according to RCC MRx RB 3251.112 rules, the material and the thickness chosen for the main vessel are sufficient to withstand the current quench EM loads. The maximum Von Mises Stress is lower than the admissible stress limit ( $S_m = 265$  MPa) in the whole main vessel.

Higher values of Von Mises Stress at the boundary nodes can be indeed overlooked. However, the attachments between ports and VV shall be evaluated by a dedicated submodel.

The equivalent stresses expected for the VV is shown in Fig. 14.

### 3. Cryostat vessel

The Cryostat Vessel (CV) is a vacuum tight container, surrounding the entire Tokamak Basic Machine, which provides the vacuum for the superconducting magnets and forms part of the secondary confinement barrier. The vacuum environment is intended to avoid excessive thermal loads from being applied to the components that are being operated at cryogenic temperatures by gas conduction and convection. The CV provides ports and penetrations, with proper bellows, to the vacuum vessel (Fig. 15).

Proper bellows compensate for differential movements. These bellows are made of stainless steel. Development of suitable bellows will be completed during more detailed design phases.

CV must also provide openings for pipes connecting equipment outside the Cryostat to the corresponding elements inside the Cryostat (e.g. magnet feeders, water cooling pipes, instrumentation feedthroughs, CV pumping systems).

CV design must allow maximum feasible personnel access inside the cryostat by having penetrations for the deployment of shielded

**B: Static Structural**  
Equivalent Stress  
Type: Equivalent (von-Mises) Stress  
Unit: MPa  
Time: 1

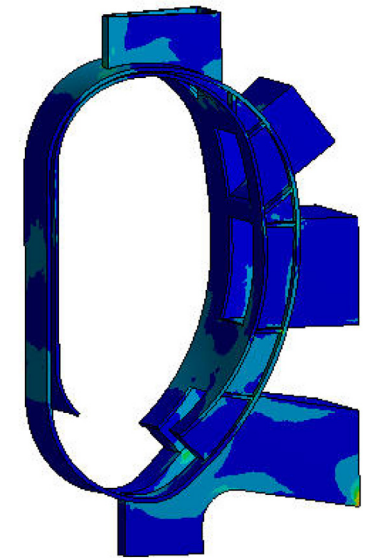
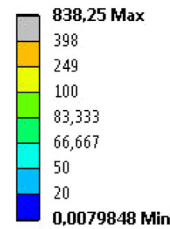


Fig. 14. DTT Vessel equivalent stress.

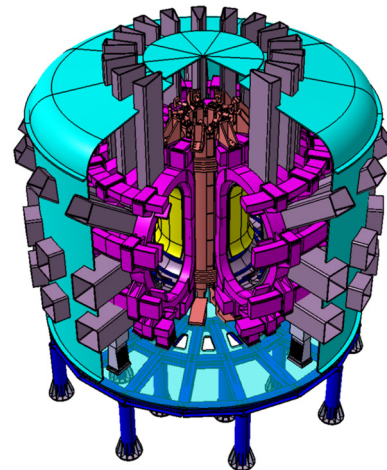


Fig. 15. Sectional view of DTT tokamak basic machine.

access ways through which personnel can access the required work locations.

The design and construction of the CV shall be consistent with providing the required vacuum for DTT. The maximum allowable leak rate shall be consistent with achieving the global leak rate requirements for the Cryostat Vacuum boundary. The maximum acceptable outgassing rate and the maximum allowable leak rate for DTT should be determined during the next design phases.

The design principles of the cryostat are chiefly based on cost minimization and functionality. The cryostat is a single-wall cylindrical vessel, with a vertical axis, a flat base and a tori-spherical top lid (Fig. 16).

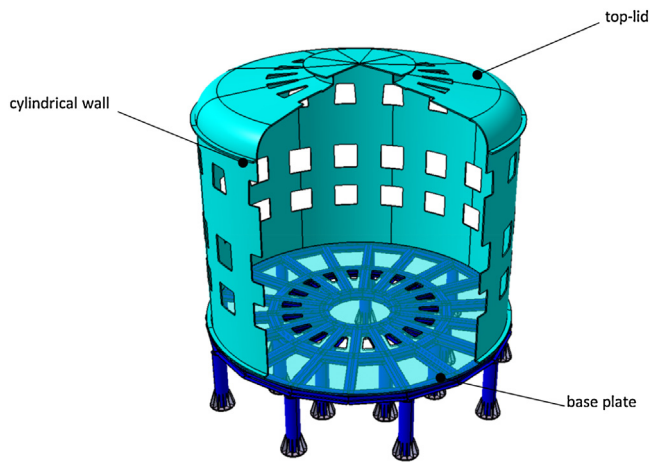


Fig. 16. Cryostat Vessel segmentation.

The weight of the top lid can be estimated in about 27 t, whilst the internal height is about 1.5 m. The cylindrical section is bolted by flanges to top lid wall at top and to base plate at bottom. Its external diameter (~10 m) is determined by the dimension of the maximum diameter of the toroidal field coil with an additional small radial clearance of approximately 800 mm to facilitate the installation of components and to guarantee proper access space for in-situ repair. The height of the cylindrical section is about 7 m; this dimension is determined by the size of components inside as well as to provide adequate vertical space for penetrations through the cryostat cylindrical shell needed to make the interconnections with external systems. The weight of cylindrical portion of the CV is about 60 t. At the current pre-conceptual stage, cryostat walls are provisionally dimensioned as 40 mm thick, while the stainless steel base plate is 60 mm thick.

The CV is a fully-welded, stainless steel (AISI 304L) vessel, with a large number of penetrations for access to VV ports at five levels and further horizontal penetrations for coolant pipe work at upper and lower levels, and cryo and current feed lines to magnets at the upper and lower levels.

Considering the top tori-spherical dome-shape lid and lower flat head, and particularly the large penetrations for the port access through the cylindrical shell, the stability against the buckling will be the main driver for the mechanical design, and cryostat structure shall be analyzed for buckling strength.

It is understood that further analyses shall be conducted to better determine steel thickness during more detailed design stages.

Furthermore, access penetrations for manned access for repair or inspection shall be included in the lower cylindrical portion of the CV for horizontal and vertical entry and in the top lid of CV for vertical entry.

Cryostat base plate is supported on a frame, which is mainly consisted of H-beams in radial and toroidal directions (see Fig. 17).

Magnets system, the vacuum vessel and thermal shields are supported on the cryostat base. The frame is mainly supported by 16 pillars of 457 mm in external diameter with the thickness of 40 mm. All H-beams are welding structure with 304L stainless steel of 30 mm thickness and 300 mm height. The height from the level of the test hall to the bottom of the frame is 2000 mm.

There are 18 H-beams in radial direction and 36 H-beams (18 short and 18 long ones) in toroidal direction. Thirty-six additional support plates (18 supports for VV, 18 supports for TF&PF coils) offer the bases for the vacuum vessel and magnet respectively. The weight of the supporting steel structure can be estimated in about 62 t.

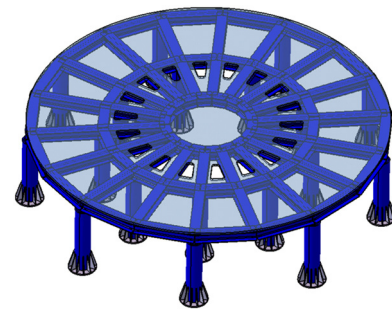


Fig. 17. Supporting steel structure.

Table 3

Main characteristics of Cryostat Vessel.

Material	AISI 304L stainless steel
External Diameter	~10 m
Internal height	~8,5 m
Wall thickness	40 mm
Top lid weight	~27 t
Cylindrical portion Weight	~60 t
Supporting steel structure	~62 t
Total weight	~149 t

An elasticity support structure was proposed. It may absorb deformation caused by bake-out and electromagnetic forces. However, stress analyses and calculations shall be conducted in more advanced design stages.

In Table 3 the main characteristics of Cryostat Vessel (CV) are summarized.

#### 4. Conclusions

The present work focused on the conceptual design of the first wall and the main containment structures of DTT fusion plant.

The work moved from the geometrical constraints imposed by the desired plasma shape and the configuration needed for the magnetic coils. Many other design constraints have been taken into account such as remote maintainability, space reservations for diagnostic and heating equipment, etc.

The basic vessel design resulted in an all-welded single-wall toroidal structure made of 18 sectors. Proper supports have been designed for the first wall, which was conveniently segmented in view of remote maintenance. This provisional model allowed evaluating the electromagnetic loads on the metallic structure of the vacuum vessel resulting from the current quench due to a plasma disruption.

A preliminary FE mechanical assessment conducted according to applicable nuclear codes showed that INCONEL<sup>®</sup> 625 can be a suitable material for vacuum vessel, but further investigations about manufacturing and costs are needed based of previous experience from already existing fusion plants.

The design principles of the cryostat were chiefly based on cost minimization and functionality; thus it was conceived as a single-wall cylindrical vessel supported by a steel frame structure. The same structure will hold the vacuum vessel and the magnets. An estimation of the expected weights was also provided.

#### Acknowledgement

This work has been carried out within the framework of the EUROfusion Consortium and has received funding from the Euratom research and training programme 2014–2018 under grant agreement No 633053. The views and opinions expressed herein do not necessarily reflect those of the European Commission.

## References

- [1] R. Albanese, H. Reimerdes, The DTT device: role and objectives, *Fusion Eng. Des.* (2017), <http://dx.doi.org/10.1016/j.fusengdes.2016.12.025> (in press).
- [2] R. Albanese, A. Pizzuto, WPDTT2 Team, The DTT proposal. A tokamak facility to address exhaust challenges for DEMO: introduction and executive summary, *Fusion Eng. Des.* (2017) (in press) <https://doi.org/10.1016/j.fusengdes.2016.12.030>.
- [3] L. Affinito, A. Anemona, M.L. Apicella, P. Batistoni, G. Calabrò, A. Cardinali, F. Crisanti, DTT: Divertor Tokamak Test Facility Project Proposal, 2015.
- [4] S. Benhard, J. Boscary, H. Greuner, P. Grigull, J. Kießlinger, C. Li, A. Vorköper, Manufacturing of the Wendelstein 7-X divertor and wall protection, *Fusion Eng. Des.* 75 (2005) 463–468.
- [5] ITER Material Property Handbook (private communication).
- [6] D. Campbell, ITER research needs, in: EUROfusion ITER Physics AWP-2016 Preparation Meeting, Garching, 6–8 July, 2015 (private communication).
- [7] R. Mozzillo, D. Marzullo, A. Tarallo, C. Bachmann, G. Di Gironimo, Development of a master model concept for DEMO vacuum vessel, *Fusion Eng. Des.* 112 (2016) 497–504.
- [8] Website: <http://www.specialmetals.com/alloys/inconel/inconel-alloy-625.pdf>.
- [9] TaoSong Yun, et al., Structural analysis and manufacture for the vacuum vessel of experimental advanced superconducting tokamak (EAST) device, *Fusion Eng. Des.* 81 (2006) 1117–1122 (8).
- [10] C. Labate, G. Di Gironimo, F. Renno, Plasma facing components: a conceptual design strategy for the first wall in FAST tokamak, *Nucl. Fusion* 55 (11) (2015) 113013.
- [11] R. Albanese, M. Mattei, F. Villone, Prediction of the growth rates of VDEs in JET, *Nucl. Fusion* 44 (9) (2004) 999.
- [12] T. Hender, et al., *Nucl. Fusion* 47 (2007) S128.
- [13] R. Albanese, G. Rubinacci, Finite element methods for the solution of 3D eddy current problems, *Adv. Imaging Electron Phys.* 102 (1997) 1–86.
- [14] F. Villone, et al., Plasma Phys. Control. *Fusion* 55 (2013) 095008.